

An Application of SAGE Algorithm for UWB Propagation Channel Estimation

Katsuyuki Haneda, Jun-ichi Takada
Department of International Development Engineering
Tokyo Institute of Technology
2-12-1, O-okayama, Meguro-ku, Tokyo, Japan
Telephone, FAX: +81-3-5734-3288
Email: haneda@ap.ide.titech.ac.jp

Abstract—In this paper, a new Ultra Wideband (UWB) channel estimation algorithm, UWB-SAGE (Space Alternating Generalized Expectation Maximization) is proposed. This algorithm is an extension of conventional SAGE algorithm which is often adopted for wideband channel estimation. The algorithm divides the measured data into individual ray paths and estimates the directions of arrival, propagation time, and the variation of the amplitude and phase during the propagation for each signal. The measurement campaign in indoor environment was conducted and it was shown that the algorithm could correctly extract the inherent propagation phenomena of the channel. The estimation result can be very useful for the design and analysis of UWB communication system, especially for the evaluation of waveform distortion and multipath effect.

I. INTRODUCTION

Recent communication requires higher data rate than ever and the UWB communication system has drawn a lot of interest as a promising scheme to realize this requirement. The application of UWB system requires knowledge of the propagation channel where the system is to be implemented. Characterization of the channel has been done by estimating the directions of arrivals (DOAs) and directions of departures (DODs) seen from the antenna aperture, and the times of arrivals (TOAs) of the waves from Tx to Rx. Channel modelling and clusterization of the potential scatterers are also important.

There have already been constructed theoretical and experimental schemes of channel sounding for wideband channels [1], [2]. The measurement is often conducted by using PN sequences and data processing is done in the frequency domain. In the modelling of collected data, it is required that the variation of transfer function within the considered bandwidth B and antenna aperture A is sufficiently small, namely, a condition

$$B \frac{A}{c} \ll 1 \quad (1)$$

must be held where c is light velocity. However, this condition is not satisfied in UWB systems.

For UWB channel estimation, Sensor-CLEAN algorithm [3] is well known. This algorithm estimates not only DOAs and TOAs but also incident waveforms, thus sequential data in time domain is necessary.

In this paper, we propose a frequency domain channel sounding scheme for UWB system, namely Ultra-Wide Band-

width Space Alternating Generalized Expectation Maximization (UWB-SAGE) algorithm. This is an extension of conventional SAGE algorithm which is often adopted for wideband channel estimation [4], [5]. Waveform estimation is not necessary because the algorithm assumes the transmit waveforms to be *known* in the receiver side and employs frequency domain processing. The frequency domain measurement is easily implemented with vector network analyzer and spatially scanning antenna [6] thus the algorithm is applicable for real environment estimation. Note that the UWB communication is deployed only for short range environment so that it is enough to consider the network analyzer based system.

II. PATH MODEL

In the ray based propagation model which is applicable for high frequency waves (also for UWB communication), it can be defined that one propagation path has DOA and TOA that does not depend on frequency, but has a frequency dependent complex gain. Herein single directional measurement model is considered hence the transfer function of one ray path $y_l(f, \phi_l, \theta_l, \tau_l)$ is expressed as

$$y_l(f, \phi_l, \theta_l, \tau_l) = \alpha_l(f, \tau_l) r_l(f) D(f, \phi_l, \theta_l) \quad (2)$$

where

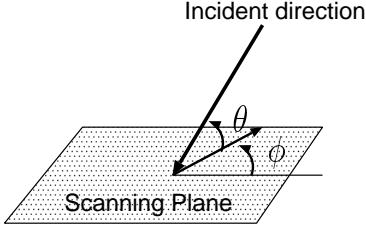
- τ_l : propagation time,
- ϕ_l : arrival azimuth angle,
- θ_l : arrival elevation angle,
- $\alpha_l(f, \tau_l)$: complex gain of the spatial propagation,
- $r_l(f)$: scattering loss,
- $D(f, \phi_l, \theta_l)$: radiation pattern of Rx antenna for a single polarization.

Note that we regard the radiation pattern of Tx antenna to be isotropic. $\alpha_l(f, \tau)$ can be expressed as the extension of Friis' Transmission Formula,

$$\alpha_l(f, \tau_l) = \frac{1}{4\pi\tau_l f} \exp(-j2\pi\tau_l f). \quad (3)$$

III. UWB-SAGE ALGORITHM

UWB-SAGE algorithm is based on the Maximum Likelihood Estimation (MLE) and has a high resolution in separating the incident waves.



$\theta : 0 \sim 90$ [deg] : Elevation angle,
 $\phi : 0 \sim 360$ [deg] : Azimuth angle

Fig. 1. Definition of Angles at Rx

A. The Data Model

Suppose that UWB channel can be expressed as the superposition of I subbands where the scattering loss and the antenna directivity within each subband is sufficiently constant. When we focus on the i th wideband channel whose center frequency is f_{ci} ($1 \leq i \leq I$), we can formulate a model for measured transfer function. Suppose there are L waves incident to uniform rectangular array (URA) in horizontal plane which has equally spaced M_1 , M_2 antenna elements in azimuth and elevation direction. The azimuth and elevation angles are defined as Fig. 1. The element spacings are Δ_x and Δ_y , respectively. By performing M_3 frequency sweeping with sampling interval Δ_f at center frequency f_{ci} , the measured transfer function y_{k_1, k_2, k_3} is denoted as Eq. (4),

$$y_{k_1, k_2, k_3} = \sum_{l=1}^L \left[\alpha_l(f_{ci}, \tau_l) r_l(f_{ci}) D(f_{ci}, \phi_l, \theta_l) \prod_{r=1}^3 e^{jk_r \mu_{l,i}^{(r)}} \right] + n_{k_1, k_2, k_3}. \quad (4)$$

where $0 \leq k_r \leq M_r - 1$ ($1 \leq r \leq 3$) indicates a index number of each sampling domain. n_{k_1, k_2, k_3} is white gaussian noise of zero mean. $\mu_{l,i}^{(r)}$ is expressed as

$$\mu_{l,i}^{(1)} = \frac{2\pi f_{ci}}{c} \Delta_x \sin \phi_l \cos \theta_l, \quad (5)$$

$$\mu_{l,i}^{(2)} = \frac{2\pi f_{ci}}{c} \Delta_y \cos \phi_l \cos \theta_l, \quad (6)$$

$$\mu_{l,i}^{(3)} = 2\pi \Delta_f \tau_l. \quad (7)$$

Plane wave approximation of the incident wave is used in this formulation.

For simplicity, we vectorize the data defined in Eq. (4) as

$$\begin{aligned} \mathbf{y}_i &= [y_{1,1,1,i} \ y_{2,1,1,i} \ \cdots \ y_{M_1,1,1,i} \ y_{1,2,1,i} \ \cdots \\ &\quad y_{M_1,2,1,i} \ y_{1,1,2,i} \ \cdots \ y_{M_1,2,2,i} \ \cdots \ y_{M_1,2,3,i}]^T \in C^M \\ &= \mathbf{A}_i \mathbf{s}_i + \mathbf{n}_i, \end{aligned} \quad (8)$$

where $M = M_1 M_2 M_3$ and \mathbf{n}_i is noise vector. \mathbf{s}_i denotes a transfer function vector that is composed of propagation and

antenna characteristics of each wave. Namely,

$$\begin{aligned} \mathbf{s}_i &= [s_{1,i} \ s_{2,i} \ \cdots \ s_{L,i}] \\ &= [\alpha_1(f_{ci}, \tau_1) r_1(f_{ci}) D(f_{ci}, \phi_1, \theta_1), \ \cdots \\ &\quad \alpha_L(f_{ci}, \tau_L) r_L(f_{ci}) D(f_{ci}, \phi_L, \theta_L)]^T \in C^L. \end{aligned} \quad (9)$$

The multi-dimensional phase difference matrices $\mathbf{A}_i \in C^{M \times L}$ is expressed as Eq. (10),

$$\mathbf{A}_i = \mathbf{A}_i(\mu_i^{(3)}) \diamond \mathbf{A}_i(\mu_i^{(2)}) \diamond \mathbf{A}_i(\mu_i^{(1)}), \quad (10)$$

where

$$\mathbf{A}_i(\mu_i^{(r)}) = [\mathbf{a}_i(\mu_{1,i}^{(r)}) \ \cdots \ \mathbf{a}_i(\mu_{L,i}^{(r)})]^T, \quad (11)$$

$$\mathbf{a}_i(\mu_{l,i}^{(r)}) = [1 \ e^{j\mu_{l,i}^{(r)}} \ \cdots \ e^{j(M_r-1)\mu_{l,i}^{(r)}}]^T, \quad (12)$$

and \diamond denotes the Kronecker product of each row of the matrices.

The UWB channel model can be derived as a simple I superposition of this subband model.

B. SAGE Algorithm

MLE estimates a component that maximize the likelihood function, which is the probability of observing the measured data by assuming that the data follows a certain distribution. In the considered signal model, the received signal is perturbed by gaussian noise. Therefore, the probability of generating the measured data vector \mathbf{y}_i from signal component vector $\boldsymbol{\mu}_i$, $p(\mathbf{y}_i | \boldsymbol{\mu}_i)$ is

$$p(\mathbf{y}_i | \boldsymbol{\mu}_i) = \prod_{k_1=1}^{M_1} \prod_{k_2=1}^{M_2} \prod_{k_3=1}^{M_3} \left(\frac{1}{\pi \sigma} \times \exp \left[-\frac{|y_{k_1, k_2, k_3, i} - \mu_{k_1, k_2, k_3, i}|^2}{\sigma^2} \right] \right) \quad (13)$$

where the noise is assumed to be independent and identically distributed.

By taking the logarithm, the maximum likelihood condition is expressed as the following minimization problem,

$$\arg \max_{\boldsymbol{\mu}} \ln p(\mathbf{y}_i | \boldsymbol{\mu}) = \frac{1}{\sigma^2} \arg \min_{[\phi_l, \theta_l, \tau_l, s_{l,i}]_{l=1}^L} \|\mathbf{y}_i - \mathbf{A}_i \mathbf{s}_i\|^2. \quad (14)$$

The required search in Eq. (14) is a simultaneous $4L$ dimensional one.

To reduce the computationally prohibitive multidimensional simultaneous search, the Expectation-Maximization (EM) algorithm is introduced [7]. This estimates the complete data $\mathbf{x}_{l,i}$ from the incomplete data \mathbf{y}_i as Eq. (15).

$$\mathbf{x}_{l,i} = \mathbf{a}_{l,i} s_{l,i} + \beta_{l,i} (\mathbf{y}_i - \mathbf{A}_i \mathbf{s}_i) \quad (15)$$

Herein the nature of the additive white gaussian noise is considered in the derivation and the initial values of the parameters are needed. $\beta_{l,i}$ is a positive number which has a constraint $\sum_{l=1}^L \beta_{l,i} = 1$ but is practically set to 1. This makes us possible to maximize the conditional Fisher information of complete data $\mathbf{x}_{l,i}$ [5]. In our case, incomplete data means the

measured data and complete data corresponds to the data of each incident waves which are not directly measured in the experiment. The modified log-likelihood function for complete data is analogous to Eq. (14),

$$\arg \max_{\boldsymbol{\mu}} p(\mathbf{x}_{l,i} | \boldsymbol{\mu}) = \arg \min_{[\phi, \theta, \tau, s]} \|\mathbf{x}_{l,i} - \mathbf{a}_i s_i\|^2. \quad (16)$$

This means that the simultaneous search dimension is reduced to 4. We can see that the search estimates the parameters of the waves which extract the largest power from the complete data. Thus, we can rewrite this minimization procedure in the following 3-dimensional simultaneous search.

$$(\hat{\phi}_l, \hat{\theta}_l, \hat{\tau}_l) = \arg \max_{[\phi, \theta, \tau]} |z(\phi, \theta, \tau, \mathbf{x}_{l,i})| \quad (17)$$

The cost function $z(\phi, \theta, \tau, \mathbf{x}_{l,i})$ is denoted as

$$z(\phi, \theta, \tau, \mathbf{x}_{l,i}) = E[\mathbf{a}_i^H \mathbf{x}_{l,i}]. \quad (18)$$

This is equivalent to finding the matched filter for a certain incident wave. The complex transfer function of the wave $s_{l,i}$ is derived from the estimated parameters as,

$$s_{l,i} = \frac{z(\hat{\phi}_l, \hat{\theta}_l, \hat{\tau}_l, \mathbf{x}_{l,i})}{M}, \quad (19)$$

and the path gain $P_{l,i} = |s_{l,i}|^2$ is obtained.

SAGE algorithm divides the whole search space of EM algorithm into hidden data spaces. In our case, the search is carried out sequentially in the following order,

$$\hat{\phi}_l = \arg \max_{\phi} |z(\phi, \theta_l, \tau_l, \mathbf{x}_{l,i})|, \quad (20)$$

$$\hat{\theta}_l = \arg \max_{\theta} |z(\hat{\phi}_l, \theta, \tau_l, \mathbf{x}_{l,i})|, \quad (21)$$

$$\hat{\tau}_l = \arg \max_{\tau} |z(\hat{\phi}_l, \hat{\theta}_l, \tau, \mathbf{x}_{l,i})|. \quad (22)$$

In this way, we can obtain updated estimates of parameters from the old ones. This process is repeated until the likelihood reaches a certain maximum value or the estimated parameters converge on some fixed value.

C. UWB-SAGE Algorithm

As explained in section III-A, UWB channel can be expressed as a set of subbands. Therefore, in the UWB channel estimation, the cost function to be maximized $z(\phi, \theta, \tau, \{\mathbf{x}_{l,i}\}_{i=1}^I)$ is a simple summation of modified log-likelihood of each subband as Eq. (23).

$$z(\phi, \theta, \tau, \{\mathbf{x}_{l,i}\}_{i=1}^I) = \sum_{i=1}^I |E[\mathbf{a}_i^H \mathbf{x}_{l,i}]| \quad (23)$$

In the use of SAGE algorithm, SIC (Successive Interference Cancellation) type procedure is preferable when the number of samples is sufficiently large [6], [8]. An example of the search procedure is depicted in Fig. 2. This scheme is a combination of local search based on SAGE algorithm and global mesh search based on EM algorithm. In global mesh search, we aim at the region which may include a maximum point of the cost function. After that, local search is carried out inside the selected region to find an accurate peak. The

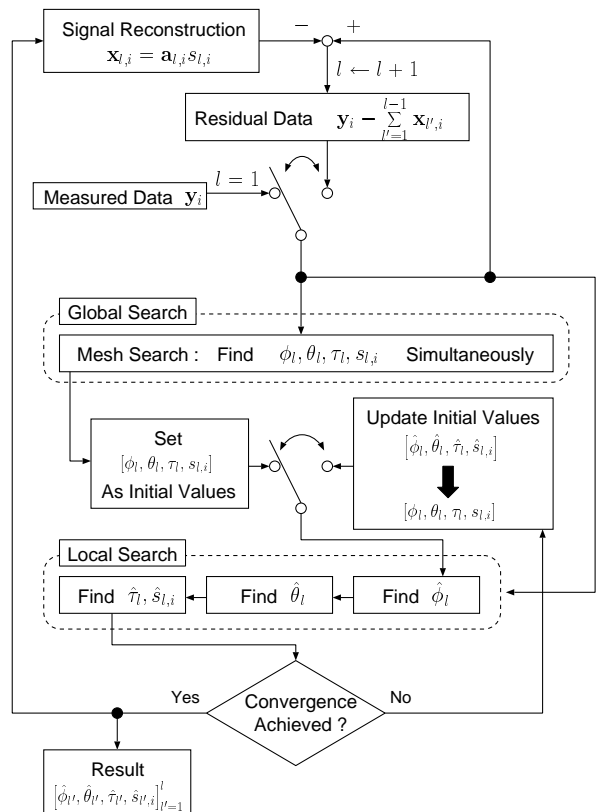


Fig. 2. Flow Chart of the SAGE Algorithm of SIC Type for each subband [8].

process is repeated until the number of detected paths reaches the predefined number of waves or the detected path level falls below the noise floor level. The transfer function of i th subband channel is obtained from Eq. (19).

It should be pointed out that the system parameters to be optimized in the estimation are the following two, which must be adjusted within the criteria of Eq. (1):

- 1) Sampling interval of frequency domain Δ_f . Δ_f gives the upper bound of arrival time without the appearance of aliasing, $\tau_{\max} = \frac{1}{\Delta_f}$.
- 2) The number of samples in spatial domain M_1 , M_2 and in frequency domain $M_3 I$. These parameters decide the basic resolution of the algorithm.

IV. UWB CHANNEL MEASUREMENT

A. Measurement System and Environment

With the UWB-SAGE algorithm and measurement system proposed in [6], we estimated typical indoor channel with UWB signal in order to assess the validity. Figure 3 is the architecture of the measurement system. The system measures the transfer function by Vector Network Analyzer (VNA) and the synthesized antenna aperture is achieved with one element antenna and spatial scanner.

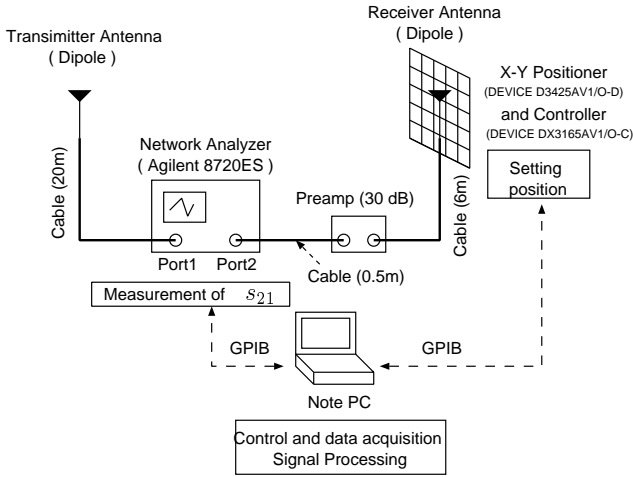


Fig. 3. UWB channel measurement system

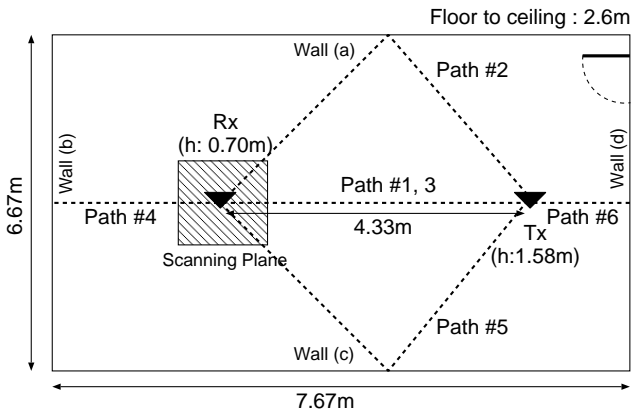


Fig. 4. Floor plan of the measurement environment and result of path identification.

The floor plan of the measurement environment is depicted in Fig.4. The Tx and Rx antennas are set in the same room with different height. The size of the room is about 6.7×7.7 [m²] and are typical small conference room. There is almost no objects in the room except for the measurement equipment. During the experiment, the door was shut so that the channel was considered to be time invariant. The specifications of the measurement and UWB-SAGE algorithm implementation is depicted in Table I. Note that the back-to-back calibration is a procedure which removes the effect of mismatch occurred between cables and antennas. In the case of executing this procedure, it should be satisfied that only direct path exists. Therefore, in the on-site calibration as our experiment, we used the electromagnetic absorber so as to isolate the Tx and Rx antennas from objects surrounded.

B. Results

Figure 5 is the averaged power spectrum obtained from the VNA. The free space gain of direct wave derived from Friis' transmission formula [10] is also shown. They have

TABLE I
SPECIFICATIONS OF THE MEASUREMENT

Bandwidth considered	3.1 [GHz] ~ 10.6 [GHz][9]
The number of samples in frequency domain	751 points ($\Delta_f = 10$ [MHz]).
Bandwidth of each subband	100 [MHz]
The number of samples in spatial domain	In horizontal plane, 10×10 points of rectangular array configuration whose intervals are 4.8 [cm](less than half wavelength in 3.1 [GHz]) Azimuth ϕ , elevation θ ,
Estimated components	propagation time τ and variation of spectrum in terms of phase and gain.
Antennas	Biconical antennas for Tx and Rx.
IF Bandwidth	100 [Hz].
Polarization of the wave	Vertical-Vertical.
Noise level of Network Analyzer	-98 [dBm].
Resolution of UWB-SAGE Algorithm	10 [deg] for azimuth or elevation, 0.2 [ns] in time domain.
Calibration	Back-to-back, the distance between Tx and Rx is 0.7 [m].

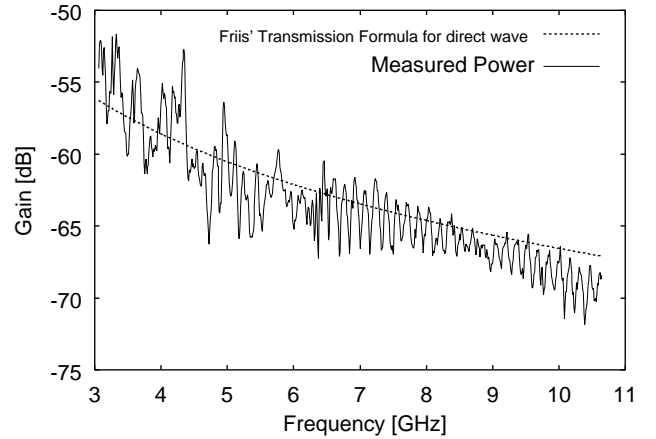


Fig. 5. Measured power spectrum and its comparison to the Friis's free space transmission formula.

small difference and it is assumed that the direct component is dominant in this line-of-sight environment. The fluctuation of the measured power spectrum is mainly due to the frequency sensitive antenna directivity.

The results of parameters estimation with UWB-SAGE algorithm is shown in Table II. There are 6 waves detected including direct paths and reflected rays from each side of the walls. In the table, parameters derived from geometrical optics method (GO) are shown as well and they agree well with the estimated ones. This means that all the waves are almost identical to the specular reflected paths. At times we can see some deviation between the estimated result and the one derived by the GO. In angle domain, this kind of error is due to the worse accuracy of endfire direction estimation.

TABLE II
RESULT OF PARAMETERS ESTIMATION BY UWB-SAGE
ALGORITHM

Path Identification	Azimuth [deg]	Elevation [deg]	Delay [ns]
#1	359.26	13.88	15.50
Direct Wave	(0.00)	(11.49)	(14.73)
#2	303.66	14.19	29.10
Wall(a) rflct.	(302.04)	(6.15)	(27.37)
#3	358.90	31.08	18.60
Ceiling rflct.	(0.00)	(34.00)	(17.40)
#4	180.90	13.07	31.70
Wall(b) rflct.	(180.00)	(5.25)	(32.03)
#5	61.92	16.72	29.50
Wall(c) rflct.	(56.00)	(6.48)	(25.98)
#6	359.33	8.57	23.00
Wall(d) rflct.	(0.00)	(8.07)	(20.91)

On the other hand, phase characteristics of the antennas could cause a bias on the delay estimation, although the effect is not significant.

The estimated spectrum of wave 1 is depicted in Fig.6. The phase shown in the figure indicates the deviation from the free space phase variation, namely in this case, the phase rotation at antennas. For the reflected waves, the phase component obtained in the estimation includes both antennas and reflection (scattering) phase characteristics.

V. CONCLUSION

We proposed an algorithm which estimates the UWB propagation channel in a deterministic way, named UWB-SAGE. This is an extension of the conventional SAGE algorithm and conducts a frequency domain processing therefore it does not require the estimation of time domain waveforms. The indoor channel measurement suggested that the algorithm could correctly separate the incident waves and evaluate the parameters of each wave.

In the processing of UWB-SAGE, antenna directivity is regarded as isotropic because of the difficulty of embedding them into multi-dimensional mode matrix \mathbf{A}_i in Eq. (8). Therefore, the estimation results include both characteristics of antenna and propagation. For the spectrum, propagation characteristics can be extracted from the estimated result by deconvoluting the effect of antenna directivity and its frequency dependence.

We must assess our algorithm in several aspect, for example, experimental verification of the resolution. The behavior of the algorithm for the estimation of waves whose delays and angles are much closer compared to the resolution is also of the interest. At the same time, several measurements not only in LOS but also in NLOS environments are needed for the aim of UWB channel modelling.

REFERENCES

[1] K. Kalliola, H. Laitinen, L. I. Vaskelainen and P. Vainikainen, "Real-time 3D spatial-temporal dual-polarized measurement of wideband radio channel at mobile station", *IEEE Trans. Instrum. and Meas.*, Vol. 49, No. 2, pp. 439–448, Apr. 2000.

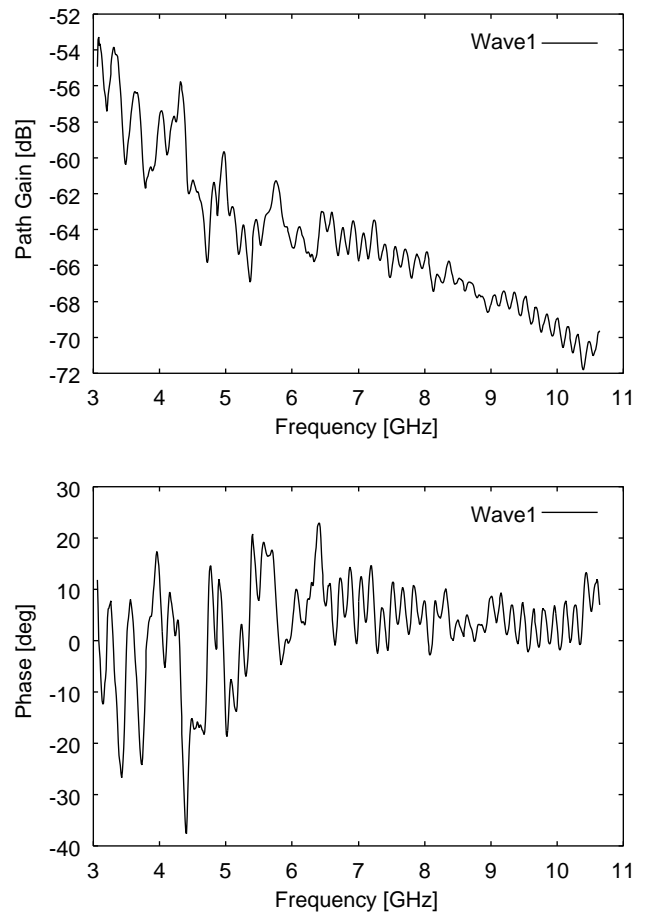


Fig. 6. Estimated gain and phase of wave 1.

[2] R. S. Thomä, D. Hampicke, A. Richter, G. Somerkorn, A. Schneider, U. Trautwein, and W. Wirthner, "Identification of time-variant directional mobile radio channels", *IEEE Trans. Instrum. and Meas.*, Vol. 49, No. 2, pp. 357–364, Apr. 2000.

[3] R. J. Cramer, R. A. Scholtz, M. Z. Win, "Evaluation of an ultra-wideband propagation channel", *IEEE Trans. Antennas Propagat.*, Vol. 50, No. 5, pp. 561–570, May 2002.

[4] J. A. Fessler and A. O. Hero, "Space-alternating generalized expectation-maximization algorithm", *IEEE Trans. Signal Processing*, Vol. 42, pp. 2664–2677, Oct. 1994.

[5] B. H. Fleury, M. Tschudin, R. Heddergott, D. Dahlhaus, and K. I. Pedersen, "Channel parameter estimation in mobile radio environments using the SAGE algorithm", *IEEE J. Select. Areas Commun.*, Vol. 17, No. 3, pp. 434–449, Mar. 1999.

[6] K. Haneda and J. Takada, "High-resolution estimation of NLOS indoor MIMO channel with network analyzer based system", in *Proc. Personal Indoor and Mobile Radio Communication 2003 (PIMRC2003)*, Beijing, China, pp. 675–679, Sept. 2003.

[7] A. P. Dempster, N. M. Laird, and D. B. Rubin, "Maximum likelihood from incomplete data via the EM algorithm", *J. Royal Statist. Soc., Ser. B*, Vol. 39, No. 1, pp. 1–38, 1977.

[8] B. H. Fleury, X. Yin, K. G. Rohbrandt, P. Jourdan, and A. Stucki, "Performance of a high-resolution scheme for joint estimation of delay and bidirection dispersion in the radio channel", in *Proc. IEEE 55th Vehicular Technology Conference (VTC 2002/Spring)*, May 2002.

[9] Federal Communications Commission, "Revision of part 15 of the commission's rules regarding ultra-wideband transmission systems", *First Report and Order*, FCC 02–48, Apr. 2002.

[10] H. T. Friis, "A note on a simple transmission formula", in *Proc. IRE*, Vol. 34, No. 5, pp. 254–256, May 1946.